J. Fluid Mech. (1969), *vol.* 35, *part* 2, *pp.* 273–298
Printed in Great Britain

Wave-number selection at finite amplitude in rotating Couette flow

By H. A. SNYDER
Woods Hole Oceanographic Institution, Woods Hole, Massachusetts

(Received 29 November 1967 and in revised form 26 July 1968)

Measurements have been made of the wavelength of Taylor vortices between rotating cylinders. It is shown that the relaxation time of such a vortex system is approximately $L^2/6\nu$, where L is the length of the vortex column and ν is the kinematic viscosity. Previous measurements reported in the literature have not been steady-state measurements because of the long relaxation time. The present data are accurate to 1 % and extend to 40 times the critical Taylor number. The variation of wavelength with Taylor number is linear and the slope is exceedingly small and negative. The non-uniqueness of wave-number observed by Coles (1965) in doubly periodic flows is here shown to occur in the rotationally symmetric case. It is argued that variational methods are inapplicable in determining the wave-number of finite-amplitude secondary flows. The experimental results show that the wave-number is determined uniquely by the initial conditions of the system. It is suggested that any method which neglects the time-dependent behaviour of the system cannot select the final state from the manifold of solutions which occur in non-linear problems.

1. Introduction

The manner in which wave-numbers are determined in non-linear stability theory has never been resolved satisfactorily. Consider, for example, the instability which occurs in the annular space between coaxial rotating cylinders. Taylor (1923) first showed that, when the angular velocity of the inner cylinder Ω_1 exceeds to a sufficient extent that of the outer Ω_2, a secondary flow sets in. At the critical Taylor number T_c the velocity field changes from one that is two-dimensional to one that is three-dimensional. This flow is composed of two parts: a mean velocity in the azimuthal direction θ, which depends only on the radial co-ordinate r; and an additional flow called the disturbance. The latter is periodic in the axial direction z and is either independent of θ or the dependence on θ is periodic. For the steady-state azimuthal velocity component we can write

$$v = \sum_{q=-\infty}^{\infty} \sum_{n=1}^{\infty} v_{0nq}(r,t) + \{v_{cnq}(r,t)\cos naz + v_{snq}(r,t)\sin naz\}\exp i(qm\theta), \qquad (1.1)$$

where q, n, and m are integers. Here, m may equal zero, in which case we may set $v_{snq} = q = 0$ without loss of generality. Velocity fields of this sort are steady for a considerable range of the Taylor number above the critical value; the extent of

this region depends strongly on the ratio of the radii of the cylinders, $\eta = R_1/R_2$, where $R_2 > R_1$.

When the complete non-linear equations are made dimensionless, it is found that Couette flow is specified by three dimensionless parameters—at least when the cylinders are infinitely long. (End effects and length effects will be treated later.) The choice of parameters is somewhat arbitrary and we will choose for the purpose of this discussion either $R_{1n} = \Omega_1 R_1^2/\nu$, $R_{out} = \Omega_2 R_1^2/\nu$ and η or R_{1n}, $\mu = \Omega_2/\Omega_1$ and η, where ν is the kinematic viscosity. If η and R_{out} are held fixed, we should expect, upon referring to (1.1), that, for the simple case $m = 0$, v_{0n0}, v_{cn0}, and a are functions of R_{1n}.

For a fixed wave-number a, model equations have been devised to calculate v_{0n0} *vs.* R_{1n} and v_{cn0} *vs.* R_{1n} when the Taylor number T is close above T_c. The experimental results are in good agreement with theory (cf. Davey 1962 and Snyder & Lambert 1966). The wave-number of the disturbance a is relatively easy to observe and any complete theoretical treatment of the problem should predict a. Yet there are several different theories of wave-number selection, and their results are not in agreement among each other or with previous experiments.

Some of the theoretical work is based on a steady-state approach which we shall show below to be inappropriate. The initial value approach to the problem, as it has been worked out to date (cf. Stuart 1960, p. 63–97; Ekhaus 1965) is based on models, asymptotic expansions and *ad hoc* assumptions and cannot, therefore, be considered to be universally valid. Its success in predicting v_{0n0} and v_{cn0} *vs.* R_{1n} at fixed a is very encouraging. But the methods developed so far are limited to dealing with one dominant mode. It is known that when calculating wave-number selection it is necessary to consider a band of possible wave-numbers.

Considering these difficulties it is appropriate, then, to use an empirical approach, such as we report here, to settle the matter in favour of one of the theories or to reject them all. The present work is an experimental investigation of the wavelengths of Taylor vortices in the finite-amplitude region of the stability diagram. The question we ask is: how is the wave-number observed in a given experiment determined?

2. Theories of wave-number selection

2.1. *Bénard convection and rotating Couette flow*

There are several theories which apply to the problem in hand; but, in every case in which they have been applied to a specific example, it has been the Bénard problem that has been studied. Fortunately, this is no great handicap for us since these theories are quite general in their formulation. The methods and also most of the results carry over to the rotating Couette problem. We must, however, describe the arrangement of Bénard convection, cite the relevant results, and then make the analogy with the double cylinder results. It appears that, if we can answer the question posed above for Couette flow, there will be no difficulty (at least in principle) in applying the result to all types of cellular instability. This is our justification for studying the Taylor problem while the theories have treated the experimentally more involved Bénard problem.

In Bénard convection the fluid is contained in a thin layer in the horizontal and extends to infinity. There is an applied vertical thermal gradient set up by heating the bottom surface and cooling the top. Only two dimensionless parameters are needed to specify the state—the Prandtl number and the Rayleigh number. (The Rayleigh number Ra is a dimensionless measure of the thermal gradient.) At small Ra there is no motion, but beyond a critical value a cellular motion appears and the flow is periodic in the two horizontal co-ordinates. It

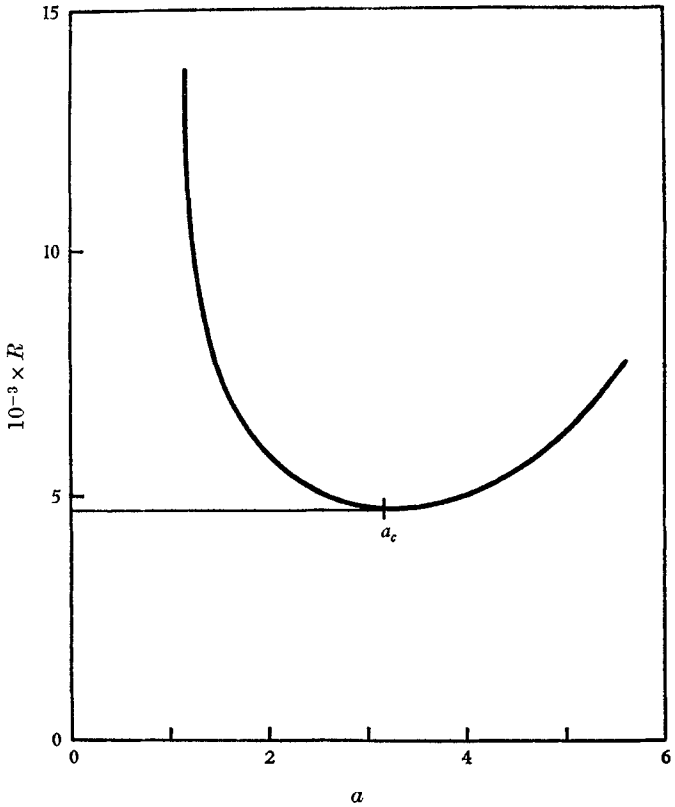

FIGURE 1. A typical Taylor number *vs.* wave-number curve at onset.

would seem that it is necessary to determine two wave-numbers. However, considerations of symmetry show that the plan-form must consist of simple geometric shapes: squares, rectangles, or hexagons. An alternative arrangement is that of rolls—a wave-form with periodicity in only one direction.

Bénard convection can be described by functions similar to the v_{0n0} and v_{cn0} of (1.1) which apply to the rotating cylinder problem. A specification of the system requires a knowledge of v_{0n0}, v_{cn0}, a and the plan-form as a function of Ra.

2.2. *Linearized results*

The results of the linearized theory are considered first. Taylor followed up his experimental work with an analysis in which he showed how the onset of

instability can be predicted by linearizing the governing equations in terms of the disturbance field. The mathematics reduces to an eigenvalue problem with the Taylor number R_{in}^2 as eigenvalue. For η and μ fixed there is an eigenvalue for each value of a. A typical curve of R_{in}^2 *vs.* a is shown in figure 1. For increasing values of R_{in} the flow first becomes unstable at a_c and this is the wave-number observed at onset.

Bénard convection is similar in most respects to Taylor's problem with one exception. The *Ra vs. a* curve looks like figure 1 and has the same interpretation. However, there are several plan-forms which are possible solutions of the governing equations and each has the same *Ra vs. a* curve. Linear theory fails to select a plan-form. In this respect Couette flow is simpler since it is fully specified at onset, except for the amplitude factor, by the linear theory.

At values of R_{in} or *Ra* greater than critical it is evident from figure 1 that there is a band of allowed wave-numbers, yet a single wave-number mode is observed. But linear theory holds only at onset and we must turn to a non-linear analysis for reliable predictions. The applicability of the linear theory close to the stability line is well substantiated. The theory and results have been reviewed in detail by Chandrasekhar (1961). Non-linear theories are not as well tested. The theoretical results derived by different methods concur on some points such as the amplitude and plan-form of the wave-form, but there has not been general agreement on even the method of calculating the wave-numbers.

2.3. *Variational methods for the non-linear problem*

Malkus & Veronis (1958) were the first to produce a theory of non-linear secondary flow with any degree of unity and completeness. Their method is a regular perturbation on the velocity and temperature fields and on *Ra*. The steady state is considered, so that all time derivatives are set equal to zero. They find that: (*a*) the plan-forms listed above are all allowed and there is no method of selecting a preferred shape using the governing equations; (*b*) the wave-number is also indeterminate. The authors suggest a criterion for selection based on an extremum principle: minimize the total heat transport (criterion I) or the mean square vertical thermal gradient (criterion II).

A new approach to hydrodynamic stability has been proposed recently by Glansdorff & Prigogine (1964). Using the methods of non-equilibrium statistical mechanics, they introduced a function of the defining variables together with their time derivatives which upon functional variation leads to equations for the pertinent fields. If the fields are expanded in a series, the lowest-order equations are identical with the linearized instability equations. The interest here is, of course, in the higher-order terms. The application of the Prigogine–Glansdorff method to Bénard convection has been carried out by Roberts (1966). In some recent work Roberts (private communication) has concluded that this method predicts a band of possible wave-numbers as Schlüter, Lortz & Busse (1965) have found in an earlier paper. No unique value of a results from this approach.

It is interesting to note that the function that is varied in the Prigogine–Glansdorff method represents a generalized measure of entropy. The extremum sought is in the rate of entropy production (criterion III). In addition to

the extremum principles enumerated above, we might add Stommel's (1947) suggestion that maximum viscous dissipation is selective, and Coles's (1965) conjecture that the preferred state is the path of steepest ascent on a surface of dissipation rate plotted against R_{in} and a. A common characteristic of the variational principles is that they are not derived directly from the governing equations and it is not known whether this is possible for any one of them.

2.4. *Methods derived from the governing equations*

The only other selection principle which we find proposed in the literature is derived from some work of Stuart (1960) and of Ekhaus (1965). Stuart has developed a perturbation scheme which differs from previous work in that the time variable is included. The initial disturbance is assumed to have the spatial wave-form predicted by linear stability theory and to depend upon time through an amplitude factor. Non-linear terms in the governing equations cause harmonic generation and contribute a correction to the mean motion. A consistent expansion is found for the mean motion, for the fundamental and the generated harmonics, and for the time-dependent amplitude. Each is a power series in the amplitude function. Thus it is possible to see how a solution to the linearized stability problem grows with time. The steady-state solution is the limit of the time-dependent wave-forms as $t \to \infty$. It has been proved that Stuart's steady-state solution with fixed a gives the same amplitude parameter as the Malkus–Veronis expansion when the same plan-form and wave-number are used. The notable feature of Stuart's method, which is of interest here, has been pointed out by Segel (1962), who suggested that the final equilibrium state must depend upon the initial state.

Ekhaus (1965) has also treated the non-linear stability problem using a time-dependent wave-form. The expansion differs from that of Stuart in that the spatial part of the wave-form is expressed in a series of the complete set of eigenfunctions occuring in the linear problem. Each of these eigenfunctions is multiplied by a time-dependent amplitude which can be determined by solving a set of non-linear ordinary equations of first-order. DiPrima (1967) has generalized Ekhaus's method so as to apply to the present problem. He also compares the formalism of Stuart and Ekhaus.

Another theoretical paper of importance for the present topic is by Schlüter *et al.* (1965). These authors have used a regular perturbation expansion about the critical point to generate a non-linear solution. This solution contains a as a parameter. The non-linear solution is then perturbed and its stability is sought. It is found that only a narrow band of wave-numbers is stable. The stable band is made up entirely of those wave-numbers predicted by the linear theory but includes only a small fraction of the total. The width of the non-linear band is of order $(Ra - Ra_{\text{crit}})$. The reader is referred to figure 1 of the cited paper for more detail. Three points are significant: (*a*) Schlüter *et al.* use a method essentially independent of the time variable in obtaining their non-linear solution; (*b*) they do not find a precise value of a at each value of Ra but instead a band of allowed values which increases with Ra; (*c*) the results are derived only from the equations of motion—no additional assumptions are required. The result of

Schlüter *et al.* of a band of wave-numbers narrower than the linearized limits is a significant achievement especially since it is derived directly from the governing equations.

DiPrima & Kogelman (private communication) have shown that the method of Ekhaus leads to a 'narrower' band for the Taylor problem. A third example of the 'narrower' band result is that of Roberts cited above. His analysis is based on a variational principle. Thus there is general agreement between the results of several different methods concerning the narrower band. It is the thesis of this paper that the selection of a particular wave-number from the allowed band is determined by the initial conditions as Segel (1962) first proposed.

I have not mentioned numerous papers concerned with finding a preferred plan-form. The Schlüter *et al.* paper leads to an unambiguous choice as does the method of Stuart. Of course, the several variational techniques also pick out a plan-form. But the double degeneracy at onset is peculiar to thermal convection and is not shared by the Couette flow problem. Therefore it is not of great concern for our present purposes. A general review of non-linear problems and the available results has been made by Stuart (1960) and by Segel (1966).

3. Previous experimental and numerical results

3.1. *Experiments on wavelengths*

Although a great deal of experimental work has been reported on both Couette flow and Bénard convection, we can find only four papers which record wavelength measurements in the finite-amplitude region. The other work on non-linear aspects of instability are concerned mainly with torque and heat flux. For the thermal convection problem Deardorff & Willis (1965) have used a convection chamber with movable walls designed so that the width to height ratio may be varied. They studied the wavelength as a function of width at Rayleigh numbers approximately 10^2, 10^3 and 10^4 times the critical value. These values of Ra are quite beyond the range where we may at present hope to compare the data with the theories described above. Our measurements on Taylor cells show that, when there are fewer than 10 cells between ends, the end effects distort the cells considerably compared with the wave-form in an infinite column of fluid. The number of cells found in the work of Deardorff & Willis is for the most part less than 10.

Coles (1965) has carried out a rather extensive investigation of the non-uniqueness of supercritical flow and the various transitions between wave-forms. Using an apparatus with $\eta = 0{\cdot}877$ and a length to gap ratio of 28, he mapped out the variables N and m as a function of R_{in} at $\mu = 0$. Here N is the number of vortices in the annulus. It may seem obvious that Coles' data may be reduced to a plot of a and m *vs.* R_{in} by dividing the length of the fluid column L by N. This, however, is not the case. We have shown in another investigation that the two vortices adjacent to the ends of the apparatus have a wave-form substantially different from that of Taylor vortices. The length of the end cell is a strong function of R_{in} and η. It is possible with a field of 22 vortices (2 end cells + 20 Taylor cells) to find the wavelength of the Taylor cells has been compressed by 10 % as R_{in} doubles owing to the expansion of the end cells. A 10 %

increase in a is equivalent to a change to 24 cells in the incorrect method of calculating the wavelength. Thus, without a separate measurement of the height of the end cells, the values of a derived from Coles' data are imprecise.

An important investigation of non-linear stability by Donnelly & Schwartz (1965) includes, among other measurements, the a *vs.* R_{in}^2 curves for $\eta = 0{\cdot}95$, $0{\cdot}90$ and $0{\cdot}85$ with $\mu = 0$. Their results were obtained by slowly increasing R_{in} above critical. The region plotted out extends throughout the region where $m = 0$. The results are somewhat difficult to interpret. We find that, within the scatter of the data, the dependence is linear and $da/dT = +7 \times 10^{-4}$, -5×10^{-4} and $-0{\cdot}2 \times 10^{-4}$ at $\eta = 0{\cdot}95$, $0{\cdot}90$ and $0{\cdot}85$ respectively. We shall show later that the method they used to find the wavelength is probably not suited for precise measurements. Some previous measurements of a by Snyder & Lambert (1966) suffer from this same difficulty. In summary it appears that there are no finite-amplitude measurements of a that are in the region where extant theories apply and that are known to a high degree of accuracy.

3.2. *Experiments on uniqueness*

It is quite well documented that the dimensionless parameters which occur in the steady-state governing equations do not determine the wave-form. For example, Pai (1943) was the first to note that in the Taylor double cylinder experiment, for $\mu = 0$ and fixed R_{in}, the wave-form is indeterminate. He showed that, depending upon the past history, the flow in his apparatus consisted of either 4 or 6 Taylor vortices for fixed R_{in}. This behaviour was evident over a wide range of R_{in}. Using hot-wire anemometry Pai measured the velocity field and showed that it differed in the two possible cases. Pai worked at very large R_{in} where turbulent effects complicated the problem. Pai's work is primarily qualitative.

Later Hagerty (1946) observed that, if the length of the fluid column L is changed while the Couette apparatus is operating in the supercritical range, the wavelength can be increased or decreased by a factor of nearly two. For both Hagerty's apparatus and that of Pai, the aspect ratio was so small that our previous measurements indicate that end effects dominate the results.

Recently Coles (1965) studied the non-uniqueness of circular Couette flow. This time the indeterminateness is shown to occur sufficiently close to the stability curve so that turbulent effects do not appear. His apparatus is long enough so that end effects do not modify the results noticeably. Using an apparatus with $\eta = 0{\cdot}88$ and for $\mu = 0$ he gives a very complete description of the mode transitions and accessible wave-numbers over a large range of R_{in} for one value of L. At values of η close to one, the $m > 0$ modes appear close above the critical value of R_{in}; there is only a small region of parameter space with two-dimensional flow ($m = 0$). All the transitions studied by Coles are between modes with $m > 0$: the flow is doubly periodic. Coles' important contribution is a table of all possible (N, m) and their transition values for fixed R_{in} over a large range of R_{in}.

Experimentalists working with Bénard convection have also noted non-uniqueness in the wave-number but more frequently in the plan-form. Here the papers of Koschmieder (1966) and Rossby (1966) are relevant. Koschmieder

is concerned chiefly with the boundary conditions and shows that end effects can determine the plan-form. This is not the type of indeterminateness considered in this paper. But it is important to know that there is another source of non-uniqueness. Rossby notes non-uniqueness of the wave-number in very carefully controlled experiments.

The question whether non-uniqueness is a property of non-linear secondary flows or may arise from end effects has been raised by several workers (e.g. Segel 1966). The author undertook to test this hypothesis by repeating experiments such as Coles (1965) describes, at several different values of L (Snyder 1968*a*). It is found that Coles's table of mode transitions is a function of L, but it is a periodic function. For example, if for L there is a transition from 24 to 28 cells at a certain R_{in}, then for a column $\frac{1}{2}L$ there is a transition from 12 to 14 cells at the same speed. This periodicity or similarity breaks down when $N \approx 10$; then end effects are important. Since Coles's L permitted 18 to 32 cells we believe that the indeterminateness exhibited by him is related to the solutions of the governing equations and not to his apparatus. The dimensions of our cylinders differ quite a bit from Coles' and the results are similar.

3.3. *Numerical results*

Several numerical experiments have been reported in which the full non-linear equations are integrated as an initial value problem. The work has been restricted for the most part to two spatial dimensions so that in the Couette case we can set $m = 0$ and in the convection case only rolls are allowed. For computations of this sort, it is not possible to use the plan-wise boundary conditions that prevail in the laboratory. One has to pick an interval for the computing grid and specify the boundary conditions at the edges. Only two choices for these conditions seem to be available. Either the ends of the interval are considered as physical boundaries or periodic conditions are imposed with the period that of the computing interval. In the former case we know from experimental experience, as we remarked above, that intervals of less than 5 wavelengths are not suitable if end effects are to be avoided. With our present computers, too many grid points are needed for extended intervals and the reported work has generally been confined to one or two wavelength strips. In the case of periodic boundary conditions it is necessary that the wave-number of the wave-form be an integral multiple of the computing interval's wave-number. If this condition is not satisfied, it is found that the calculated wave-form is not periodic and accordingly is unphysical.

There is one paper in which this problem is attacked: Meyer (1966). Meyer considers rotating Couette flow with $\eta = 0{\cdot}83$ and assumes periodic boundary conditions in the axial direction. He varies the length of the computing interval until the wave-form becomes periodic. With this method he is able to select a wavelength. He finds that this wavelength is not the one which maximizes the torque (or equivalently the heat transport). It is also not the wavelength which maximizes the growth rate. The results exhibit a lack of uniqueness which depends upon the initial perturbation.

An undesirable feature of Meyer's work is his choice of η. It is known from Coles' (1965) work that for $\eta \approx 0{\cdot}85$ the modes $m > 0$ occur about 25 % above critical R_{in}. Therefore the calculations in question, which are limited by the restriction of two-dimensionality to modes $m = 0$, are applicable only over a short range. The computations were carried to about $4R_{\text{in}}$. Snyder & Lambert (1966) have shown that the $m > 0$ modes do not occur until about $10R_{\text{in}}$ when η is as large as $\frac{1}{2}$. Thus, for two-dimensional treatments, $\eta = \frac{1}{2}$ is a more reasonable value with which to work.

4. Statement of the problem

The theories described in §2 and the experimental facts enumerated in §3 are sufficient to allow one to draw the conclusions which we hope to establish: (*a*) there is a band of allowed wave-numbers at values of R_{in} above critical and the width of the band increases with R_{in}, where the width of this band is smaller than that given by linear theory; (*b*) the selection of a wave-number from the band is determined by the initial conditions; (*c*) end effects are relatively unimportant in this process; (*d*) extremum principles are not necessary for wave-number selection and probably are at variance with the observed results. The theoretical work of Schlüter *et al.* (1965) and Ekhaus (1965) proves (*a*), while Segel's (1962) preliminary work suggests that (*b*) is reasonable. Both Meyer (1966) and the present work contribute to show (*d*) to be true. The experiments of Coles on (*a*) and (*b*) and of Snyder (1968*a*) on (*c*) furnish conclusive proof of these points.

Be that as it may, many people working on fluid dynamics do not appear to be convinced of the point of view summarized in (*a*)–(*d*). In evaluating his data, Coles (1965) does not draw the conclusion (*b*) but develops a statistical explanation. There is need for a deliberate set of experiments to examine these points explicitly and in detail, and then to make the logical synthesis. This is one purpose of this paper. The other is to provide some highly accurate measurements of a which can be checked analytically and numerically.

In the next section the precautions necessary to get accurate wavelength measurements are described. This is followed by data on item (*b*). Section 7 deals with item (*a*), and here the actual measurements of a are presented. The paper ends with a discussion of non-uniqueness illustrating its interpretation in terms of the governing equations and some implications of the results for statistical mechanics.

5. Apparatus and preliminary experiments

5.1. *Apparatus*

The equipment has been described several times in the past: Snyder & Karlsson (1964), Snyder (1968*b*). Accordingly, it is sufficient to state: $R_1 = 3{\cdot}140 \pm 0{\cdot}001$; $\eta = \frac{1}{2}$; the maximum axial working space of the annulus is 95 cm; the apparatus is held isothermal to ± 5 mdegC; the fluid is an aqueous solution of glycerol; flow visualization is by the aluminium flake method using a concentration of about 5×10^{-2} g/l.; thermistor anemometers (Lambert, Snyder & Karlsson 1965)

measure the shear at the inner cylinder. Figure 2 is a schematic of the optical system which has been added for these experiments. Parallel light from the left passes through a slit and illuminates an axial plane of about 2 mm thickness. The lighted plane is viewed at right angles by an observer with a cathetometer. An

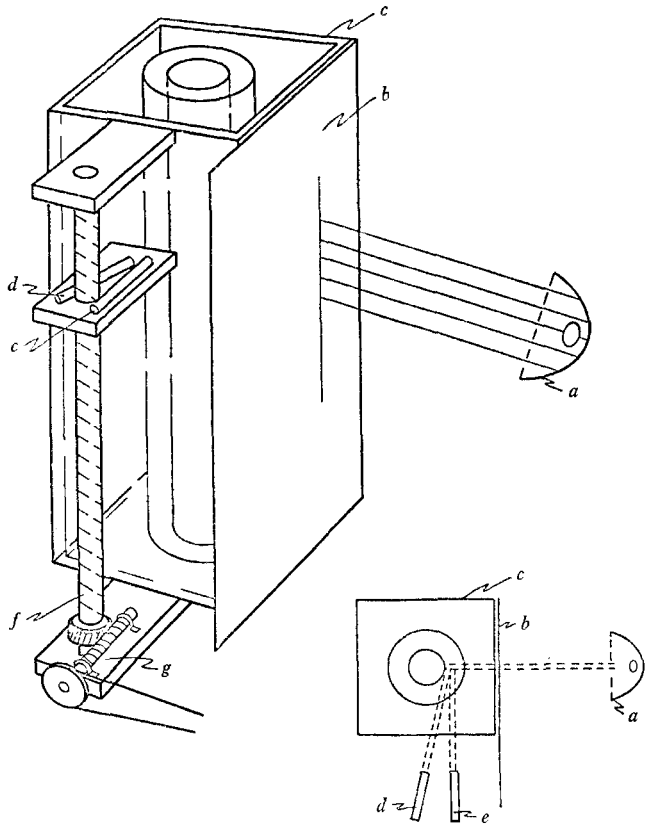

FIGURE 2. A schematic of the optical equipment: *a*, light source and parabolic reflector; *b*, light shield; *c*, Lucite outer cylinder; *d*, photocell; *e* light source for photocell; *f*, lead screw; *g*, worm drive.

alternative method is shown in the figure. It consists of a photocell at one focus of a telescope which has as its conjugate plane the lighted surface. The photocell is attached to a lead screw borrowed from a lathe and can be scanned up or down at constant speed. A light source for the photocell moves along with the scanning head and is always focused at the same point as the photocell telescope. The alignment of the aluminium flakes produces sharp peaks in the output of the photocell as the line of sight passes cell boundaries.

The choice of $\eta = \frac{1}{2}$ is dictated by the desire to have available a large area of parameter space in which the spatial variation of the field is two-dimensional, i.e. $m = 0$. This facilitates both numerical calculations and analytic computations of t he expected results. Analytic methods such as those of Stuart can be

applied to the case $m = 0$ (cf. Davey, DiPrima & Stuart 1968), but the complexity of the equations which ensue is not conducive to rapid progress. Our prime objective in this research is to complement the theoretical work on nonlinear mechanisms and it is highly important that our results be in a form that can be compared with predictions. Hence the restriction to the area $m = 0$.

5.2. *Experimental problems*

Previous data on wave-number measurements in the finite-amplitude region show a rather large scatter: Snyder & Lambert (1966), Donnelly & Schwartz (1965). This is due in part to non-uniqueness, but the onset wavelength, which is unique, still shows a large spread (cf. Taylor 1923 and more recent data by Donnelly & Fultz 1960). It seems reasonable, considering the instruments involved, that, if the wavelength data are repeatable, the errors should not be more than 1%. A search for the source of the trouble led us to ask three questions: (*a*) how long must one wait after the values of R_{in} and R_{out} become constant until the wave-form has reached a steady state; (*b*) do all the cells have the same wavelength or is there a gradual trend near the ends; (*c*) how great is the scatter from run to run?

All these questions can be answered by using the photocell device described above with the following procedure: the case $\mu = 0$ is used for all the data in this section. The inner cylinder is suddenly started rotating and the photocell is scanned up and down the length of the column repeatedly. The time scale of the readjustments being measured is small compared with the time for one traverse of the scanning head. There are fiducial marks in the line of sight of the photocell which obstruct the view and are recorded as sharp pulses in the photocell output. The fiducial pulses calibrate the recorder chart in terms of distance along the cylinder and allow one to measure both the wavelengths and the motion of a particular cell wall with respect to the end of the apparatus. Wavelengths and relative motions are measured directly from the chart recorder.

Another method is to sight the cathetometer on a chosen cell wall and to record its motion as a function of time. When the steady state is reached, the wavelength of the cell can also be measured with the cathetometer. In general, both methods are used for all readings and the data are compared as a cross-check on accuracy.

In figure 3 we show the results of two different runs with the length of the fluid column somewhat lower for the lower curve on the graph. A wavelength consists of two cells and there is a total of 22 cells in the column for these runs. The data points marked × are taken from scans made 1 min or about 25 revolutions after the start of rotation, while the points marked ○ are measured 20 min after time zero. Two facts are evident: (*a*) the cells do not all have the same wavelength when they are formed, but become more so as time progresses; (*b*) the adjustment process takes a long time.

5.3. *Measurements of adjustment time and uniformity*

A large number of runs such as those of figure 3 were made under varying conditions. Several end conditions were tried: solid end plates attached to the inner cylinder; then attached to the outer cylinder; a free surface at the top; and a semi-free surface at the bottom consisting of immiscible layers. The end boundary conditions seem to affect only the boundary cell at each end in as far as wavelength measurements are concerned (however, see Snyder 1968*a*). This result holds for all the data to be described below.

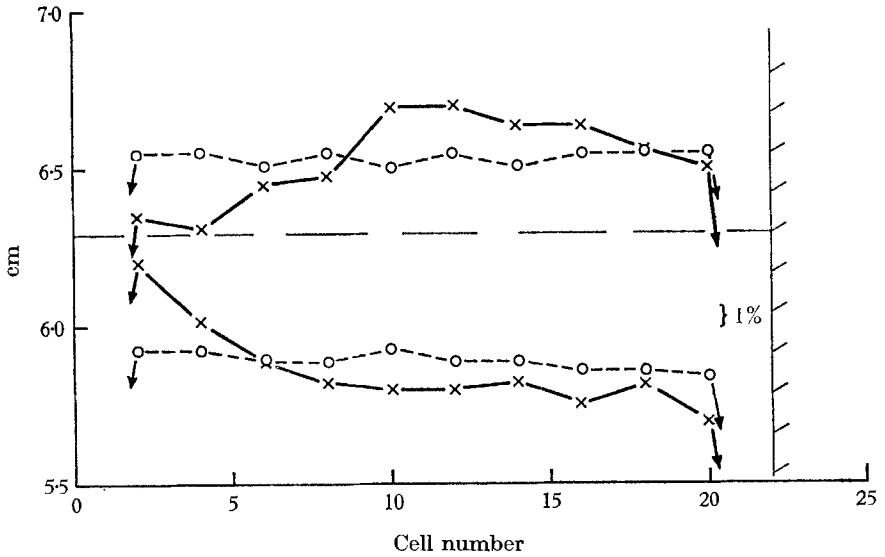

FIGURE 3. Wavelength as a function of axial distance along the cylinder. ×, initial values; O, steady-state values.

Another variable to consider is the mean wavelength to gap ratio λ/d. This parameter can be changed by using different lengths L of working fluid: Hagerty (1946), Snyder (1968*a*). The number of cells must be an integer. This, combined with non-uniqueness, allows λ/d to be varied by 20 % or more. The uniformity of λ, the adjustment time and the reproducibility of the data are not dependent perceptibly on λ/d.

The scatter in the initial non-uniformity of the cells, the × points of figure 3, seems to be random from run to run and under varying end and length conditions.

Measurements were made to determine how the adjustment time τ varied with ν, L and R_{in}. We find $\tau = C\nu/L^2$, where C is a constant, fits the data quite well. The initial and final values of R_{in} do not influence the adjustment process. This is illustrated in figure 4. Here ν and L are fixed for all the runs and the two numbers on each curve are the initial and final values of R_{in}. For this apparatus onset occurs at $R_{\text{in}} = 69$. In the next figure 5 the data of figure 4 are replotted in normalized form and a curve $dA/dt = C_1(A - A^3)$ has been fitted through the point marked with an arrow. No physical significance is attached to

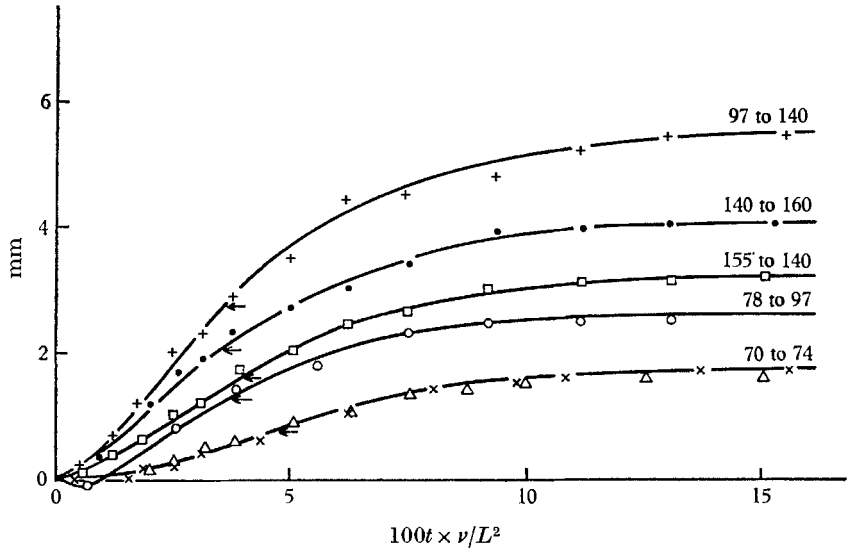

FIGURE 4. Adjustment of a cell boundary as a function of the dimensionless diffusion time. The numbers on each curve are the initial and final value of R_{in}. The abscissa is the *change* in the width of a cell.

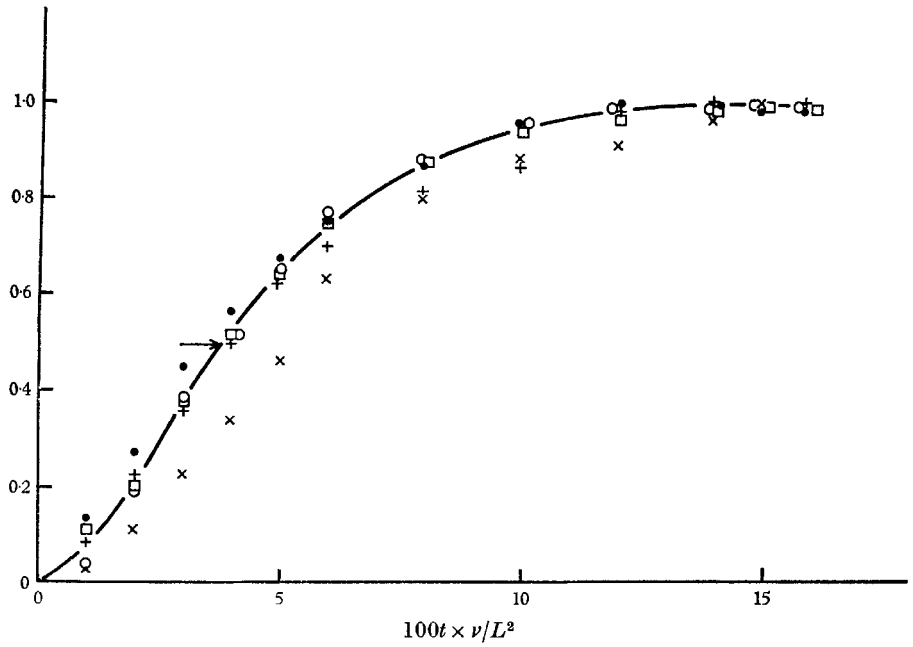

FIGURE 5. The data of figure 4 in normalized form.

this form of the equation. In figure 6 we illustrate that curves of the same general shape apply over a wide range of ν and L^2. The extreme ratios of ν and L^2 are 4·5 and 7 respectively. Figure 6 is derived from four graphs of the form of figure 5.

We have tried to indicate in figure 6 that one must wait about $0{\cdot}15L^2/\nu$ seconds after starting the apparatus before a steady state is reached. No explanation of the curves or their slight deviation from one another is made other than that L^2/ν is the diffusion time based on the length of the apparatus. It is obvious that the

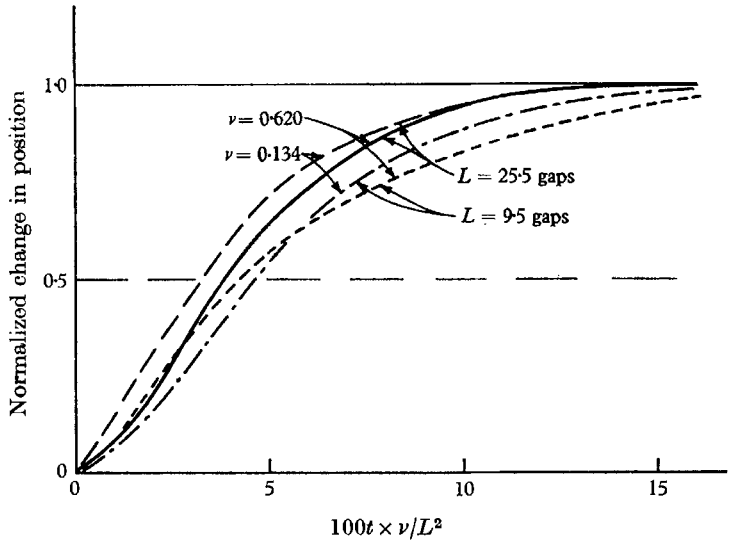

FIGURE 6. The normalized adjustment as a function of the dimensionless diffusion time for two different kinematic viscosities and lengths of the fluid column.

diffusion time across the gap d^2/ν is much less than the spin-up time $(L^2/\nu\Omega_1)^{\frac{1}{2}}$ (Greenspan & Howard 1963), which in turn is, for the R_{in} considered here, considerably less than L^2/ν. The process of adjustment is definitely diffusion and involves all the cells throughout the length of the column.

When the L and ν of various apparatus described in the literature for measuring λ are inserted into $0{\cdot}15L^2/\nu$, we note that the steady state is not reached for periods of from hours to days. It is necessary to use a high-viscosity fluid to make precise measurements in a reasonable time. This point was not appreciated in the past and a survey shows that all past measurements of λ are open to this criticism. We can expect, on this account, to find a spread in the older data about as much as the $\times$ data of figure 3. Any change in the conditions of the apparatus such as the continuous flow used by Snyder & Lambert (1966) to move the cells past the sensor, or the motion of the sensor itself as in Donnelly & Schwartz (1965), will prevent the attainment of steady state and lead to scatter. In the present research we used $\nu \approx 2$ C.G.S. units and $L \approx 80$ cm so that the waiting time is about 10 min.

Returning to the question of the uniformity and reproducibility of cell widths, the data show that, if one waits the requisite time, the cells, with the exception of the two boundary cells, are uniform in λ to better than 1 %. The values of λ with L and R_{in} fixed vary by less than 1 % from day to day.

6. Experiments on uniqueness

6.1. *Attaining a desired wave-number*

The wavelength which is observed when R_{out} is fixed and R_{in} is slowly increased through critical is close to the value predicted by the linearized theory. The discrepancy is due to the quantization of the cells. There are two boundary-layer cells—one at each end—and the intervening column is divided up into an integral number of cells $(N-2)$. The spacing is uniform and N is chosen to make λ as close as possible to the calculated value.

In another study we investigated the end cells and found that their character depends on whether the boundary is non-slip (solid) or a free surface. (The latter includes the semi-free interface between immiscible liquids.) At a non-slip boundary the height of the cell is a function of R_{in} but almost independent of L or λ/d. The free surface cell has nearly opposite behaviour; it can adjust its length from about $\frac{1}{2}d$ to $2d$ in order to accommodate the Taylor cells. For both boundary conditions the cell height is a strong function of μ. The non-slip cell is driven by the Ekman layer and has the direction of circulation appropriate to close the layer. The free surface cell can have either direction of circulation when the curvature of the surface is small (small Froude number). At high rates of rotation the free surface is driven by the surface curvature and the circulation is determinate. When top and bottom end conditions are non-slip and symmetrical, there can be only an even number of Taylor vortices since the cells must mesh their swirls. If one surface is free, either an even or odd number of vortices are found; but at higher speeds there is no choice. Knowing L, the height of the non-slip cell *vs.* R_{in} and the calculated value of λ, it is possible to predict the observed λ for a slow traverse of the stability boundary.

With reference to figure 1, we expect the linearized wavelength to appear when the stability curve is crossed very slowly. This follows, since at onset the linearized value is the only unstable wavelength; its amplitude at time zero is always larger than that of any others. The first wavelength to appear is stable for a large range of R_{in}, probably because of the quantization condition and the inherent stability indicated by Schlüter *et al.* (1965). By crossing the stability boundary slowly at a point with $\mu \neq 0$ and then traversing paths in parameter space as shown in figure 7, it is possible to go to a point such as $(R_{\text{out}} = 0,\ R_{\text{in}})$ with different wavelengths. The numbers in the figure refer to the N occurring in our apparatus for one value of L. The step-by-step process is illustrated for the case of $N = 26$. Start with R_{in} and R_{out} such that the system is at point (a) just below the instability curve. Increase the speed of the inner cylinder to the point (b). Reduce the speed of the outer cylinder until $R_{\text{out}} = 0$ and the system is at point (c). To get $N = 22$ start at point (d). This type of behaviour has been exhibited for varying lengths L and varying final points ○ (refer to figure 7). The non-uniqueness arises from the large range over which each wave-number is stable. It may be difficult to compare theoretical results based on a continuous variation in λ with experiment owing to the quantization condition.

6.2. *Test of the initial value hypothesis*

The crucial test of the initial value hypothesis is the following experiment. Bring the system to the point ○ in figure 7 with 26 cells. Reduce R_{in} to a point below critical such as that marked with a triangle. Then bring R_{in} back to ○ impulsively. This manœuvre can be carried out with two motors and a mechanical differential. One motor rotates the system at speed $R_{\text{in}} = ▲$; the second motor drives the differential and adds the difference to give ○.

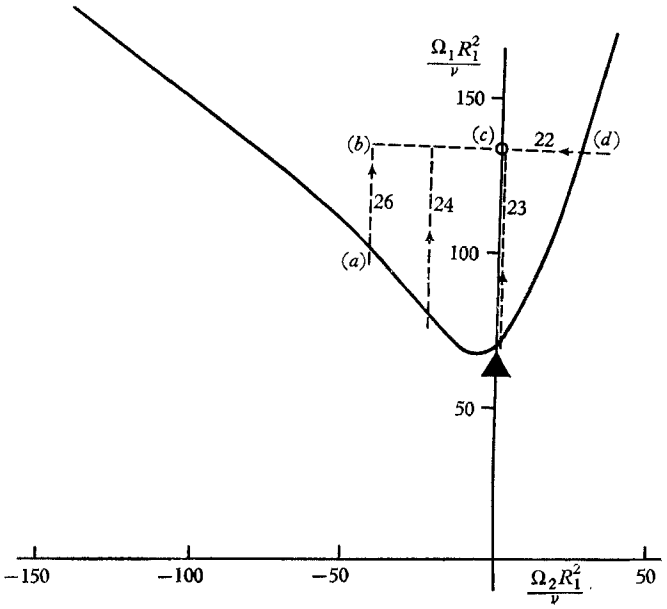

FIGURE 7. Paths in parameter space used to attain a desired wavelength. The numbers on the paths are the number of cells in the fluid column.

The results of the experiment depend upon how long the system remains at ▲. If the 26 cell disturbance has died out before the speed is increased to ○, then the final waveform has 23 cells, the linearized value. However, if there is still a measurable amplitude of the 26 cell wave-form when the speed is changed ▲ → ○, then the final cell number is 26. The amplitude of the cellular motion is measured with a thermistor anemometer. Experiments such as this have been carried out starting with 22, 24 and 26 cells with one value of L. Of course the cell number in question must be stable at ○ in order to carry out this process. Similar sequences have been investigated at other values of L and other final values of R_{in}. The results are always the same: the mode having the highest amplitude initially prevails. The data are quite reproducible from run to run and day to day.

It is also observed that one can change the values of R_{in} and R_{out} rather abruptly and throughout large areas of figure 7 and still retain the same value of N. Coles (1965) has given ample data to illustrate this point. The difference between the present data (for which $\eta = 0{\cdot}5$) and Coles's results (for which

$\eta = 0{\cdot}88$) is that he reported non-uniqueness only when the flow is doubly periodic while all the results reported in this paper are for $m = 0$, the singly periodic case.

7. Wavelength measurements

7.1. *The band of allowed wave-numbers*

The experimental methods of §5.1 were used to measure wavelengths as a function of R_{in} with $\mu = 0$. For the first set of data the upper surface is free; the lower surface is non-slip and is attached to the inner cylinder. The length of the apparatus is chosen to accommodate 22 Taylor cells having the linearized wavelength, plus an Ekman-layer cell whose height is appropriate to the critical value of R_{in}. This turns out to require $L = 23{\cdot}2$ gap widths. As R_{in} increases, the Ekman cell grows in height and the space available for the Taylor cells decreases. Some of the decrease in the observed wavelengths is due to the growth of the non-slip cell, and the remainder is absorbed by a stretching of the free surface cell. The measurements are graphed in figure 8.

To get a state such as $N = 26$ in figure 8, the procedure illustrated in figure 7 and explained in §6 is carried out. Figure 8 shows where the point ○ must be in figure 7 to attain a desired N. For example, by starting the apparatus properly and ending the sequence at $R_{\text{in}} = 100$, the states $N = 22$ to 27 can be set up; at $R_{\text{in}} = 150$ the range of N is 23 to 27; while, at $R_{\text{in}} = 200$, N can be 24, 25 or 26. Once the system is on one of the lines of constant N it remains there even if the value of R_{in} is changed violently, unless the change in R_{in} is such as to put the system beyond the range of the constant N line as shown in figure 8. The arrows indicate the transitions between states when R_{in} is increased or decreased beyond the value for which a particular value of N is stable. Transitions near $R_{\text{in}} = 200$ for $N = 27 \rightarrow 26$ and $N = 25 \rightarrow 24$ and 26 are probably due to the requirement that the number of cells be even at high values of R_{in} to meet the end conditions.

Six items of interest for wave-number selection may be noted upon studying figure 8. (*a*) The onset wavelength is unique. If R_{in} is decreased slowly to its critical value, the number of cells always changes over to 23 (as the arrows indicate in the figure) regardless of the initial value. (*b*) The width of the accessible band of a increases rapidly near critical and has a maximum at about 1·5 critical. (*c*) The extent of the band is unsymmetrical about the linearized value; the band width increases primarily on the side of increasing a. (*d*) There is a decrease in the range of accessible values of a for large values of R_{in}. This is dictated in part by the end conditions, which require an even number of cells at high rates of rotation. However, one might expect to find a state of 28 cells and this mode was sought in vain. Perhaps $N = 28$ is outside the 'narrower' band throughout the range R_{in}, but the theory indicates that the band widens as R_{in} increases. Modes with both 24 and 26 cells change to modes with $m > 0$ beyond the region where the data are plotted. It is believed that these transitions are due to end effects. (*e*) The transitions indicated by the arrows in the direction of increasing R_{in} cannot be explained by either Segel's (1962) results or the work of Schlüter *et al.* (1965). (*f*) The dependence of a *vs.* R_{in} is linear within the limits of error of the data. All

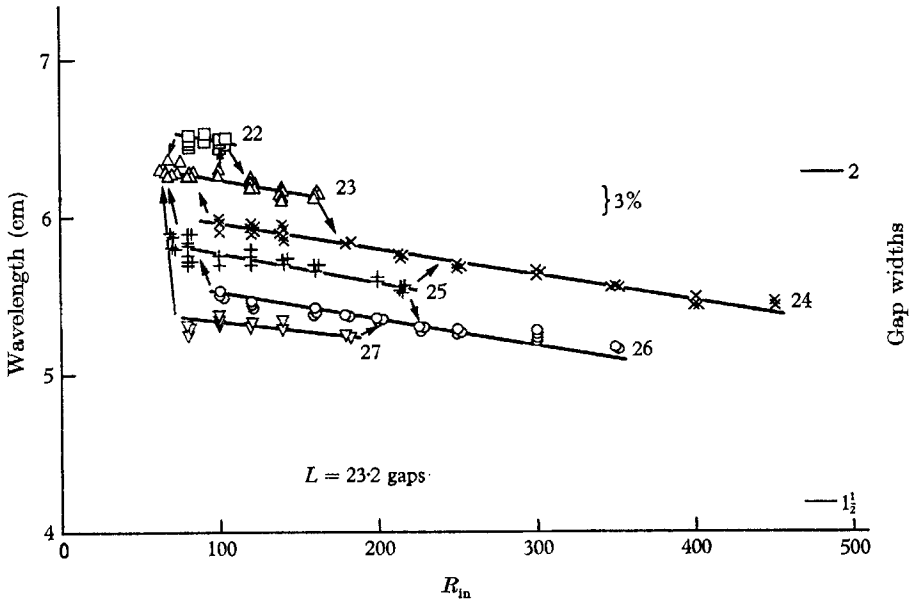

FIGURE 8. Wavelength *vs.* R_{in} plots with a non-slip boundary attached to the inner cylinder and a free surface boundary. The numbers on the curves refer to the number of cells in the fluid column.

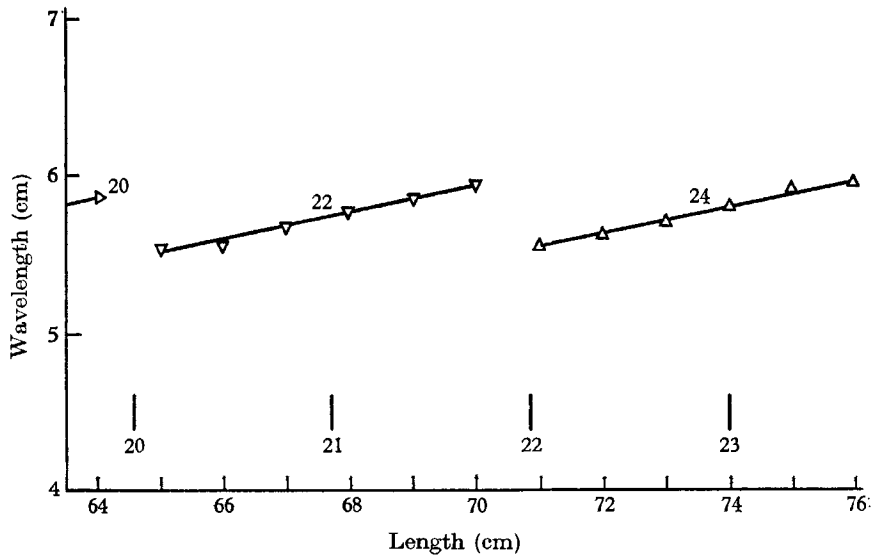

FIGURE 9. Wavelength of Taylor vortices as a function of height of the fluid column.

the slopes of $d\lambda/dR_{\text{in}}$ in figure 8 are about equal except the one at shortest λ. Corrections to be applied later will not change this last result.

7.2. *End effects and length effects*

The results of another experiment are illustrated by figure 9. The inner cylinder is rotated at $R_{\text{in}} = 300$ with $\mu = 0$. The fluid level is set at 76 cm and the number of cells is 24. The end conditions are the same as the previous example. The level is dropped by 1 cm, the apparatus is rotated for 1 h, and both the number of cells

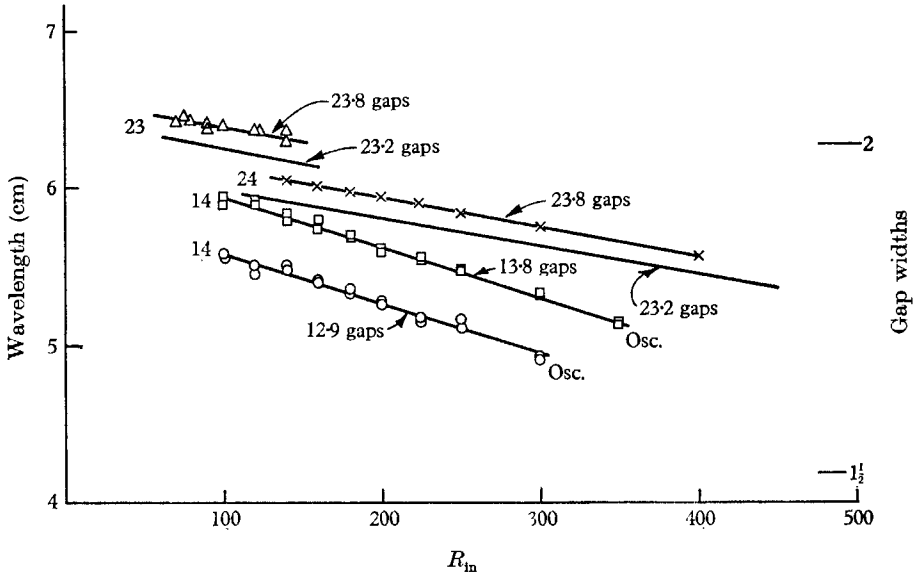

FIGURE 10. Wavelength *vs.* R_{in} plots with a non-slip boundary attached to the inner cylinder and a free surface boundary at several different heights of the fluid column.

and the wavelength are measured. This process is repeated. It is seen that the wave-number is again unsymmetrical about the linearized value, here indicated at the bottom of the graph. Figure 9 gives us a measure of the width of the allowed band at $R_{\text{in}} = 300$. The periodicity of the transitions and the equality of the slopes shown by the data indicate that end effects are not too important in these measurements.

It is reasonable to ask how a diagram such as figure 8 is modified by a small change in L and by a large change in L. Using the same conditions as for figure 8 except that L is now 23·2 gaps, the curves for 23 and 24 cells were remeasured. The plots may be seen in figure 10. The data at 23·2 gaps are also drawn in for comparison. The level was again changed and two more sets of data were taken as indicated. The useful conclusions one can draw by comparing figures 8, 9 and 10 are as follows: (*a*) The slopes and ranges of the wavelength curves are not modified by small changes in L. (*b*) When the wavelength gets to be more than about 10 % below the linearized value, the slope of $d\lambda/dR_{\text{in}}$ decreases rapidly; otherwise the slope is nearly independent of N. A discussion of the 'short wavelength' modes can be found elsewhere (Snyder 1968*a*). (*c*) For the data lines with constant

slope (i.e. excluding 'short modes'), if a correction is applied for the decrease in the column due to expansion of the Ekman cell, all slopes are equal.

This last point requires more explanation. Look at the lines in figure 10 with $L = 13{\cdot}8$, $N = 14$ and $L = 23{\cdot}2$, $N = 24$. They have different slopes. Since the increase in the height of the boundary cell is independent of L it affects the $N = 14$ slope more than the $N = 24$ line. If we consider the part of the column above the end cell and correct the wavelength for the gradual decrease of this column by using figure 9, then the corrected slopes have the same value.

To illustrate this point in a different way, we have repeated the experiment of figure 8 with the base of the annulus attached to the outer cylinder. The boundary conditions now require an odd number of cells at high rates of rotation. Thus we chose $L = 23{\cdot}2$ gaps and $N = 23$. In figure 11 the two curves are compared. Our previous measurements indicate that the height of the Ekman cell for the base 'attached outer' is almost independent of R_{In}. Thus, no correction is needed to the upper curve of figure 11. Now we may correct the data of base 'attached inner' (of figure 11) or equivalently of figure 8 as suggested and the result is shown in figure 12.

In figure 12, which is to a larger scale than the previous figures, C is the measured slope and B the slope for 'attached inner' after correction. Comparing A and B we find that within the limit of error they are equal. We hope we have convinced the reader that length and end effects can be circumvented and that the slope given by A or B is a property of Taylor vortices. The derived slope, as we mentioned, is nearly independent of N and has a value

$$d(\lambda/d)/dR_{\text{in}} = -9{\cdot}96 \times 10^{-5} \pm 5\,\%,$$

an exceedingly small rate of change.

7.3. *Error analysis*

The wavelengths are about 6 cm and we generally measured 1, 2 and 4 wavelengths from one common cell boundary. The data were always checked for internal consistency; the ratio of wavelengths in the set had to be in the ratio of 1:2:4 within 2 % or the data point was rejected. Again, the data derived from cathetometer observations were required to agree with the photocell data to within 2 % or the measurement was rejected. The cells were viewed at 90° incidence so that refractive effects should be small. Since the cathetometer can be focused and read to about $\pm 0{\cdot}02$ cm, we suspect that our accuracy is better than 1 %. Fluctuations in the speed of rotation are held to about 0·2 %. The thermal regulation is good to about ± 5 mdegC. The spread of the data points decreases as R_{in} increases. Thus we feel that the scatter near critical is due to statistical fluctuations augmented by the difficulty of focusing on the cell boundary, which becomes more diffuse as critical is approached. The precision of all the wavelength measurements is estimated at $\pm 1\,\%$.

It may be questioned whether the various modes with different N in figure 8 are really stable with respect to each other within the ranges indicated on the graph. Tests have led invariably to an affirmative answer. The mode with $N = 27$ was set up at $R_{\text{in}} = 180$ (an extreme case) and the apparatus was run

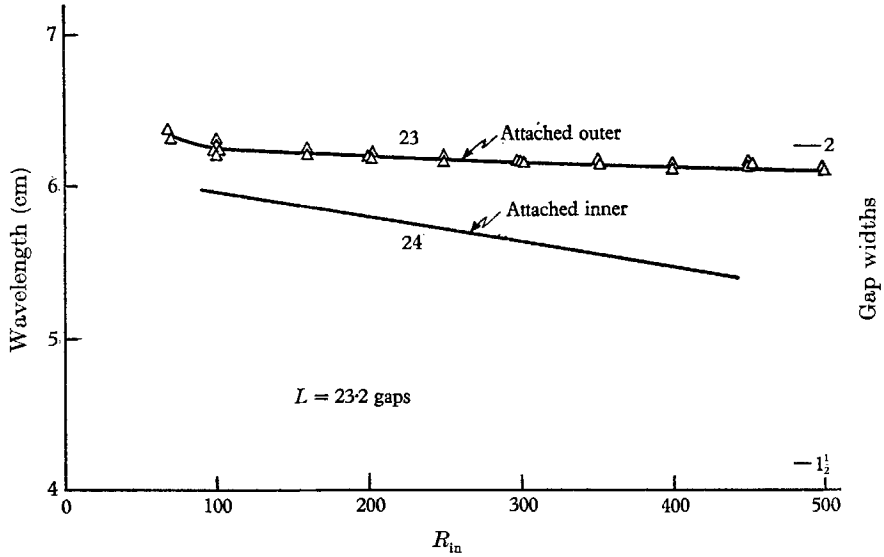

FIGURE 11. A comparison of wavelengths when the upper surface is free and the bottom surface is a non-slip boundry attached either to the inner or to the outer cylinder.

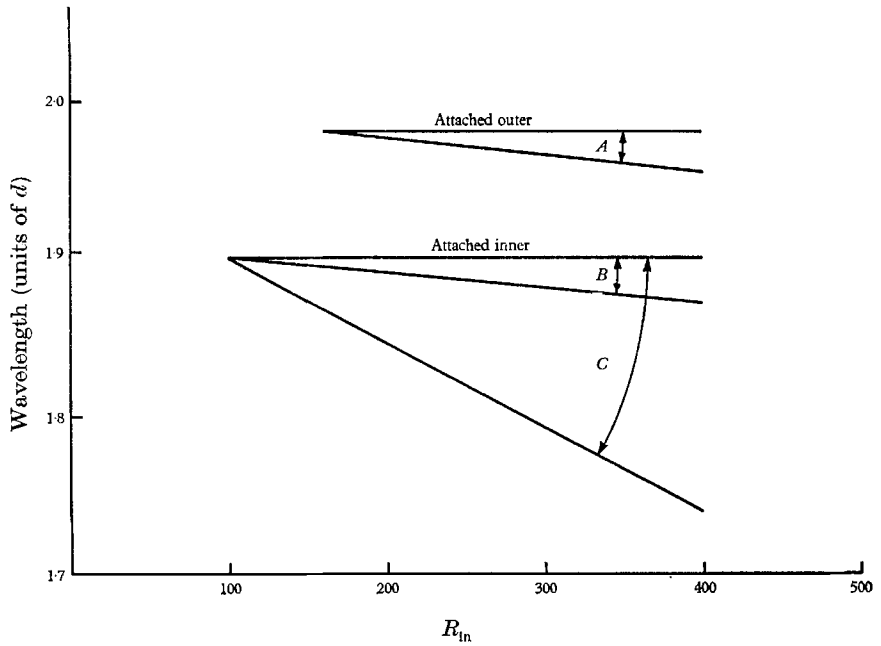

FIGURE 12. Wavelength *vs.* R_{in} curves with corrections for the change in the height of the fluid column available to the Taylor cells.

for 24 hours. No change of modes occurred. Experiments of this sort were carried out for periods of 16 hours at $N = 22$, $R_{\text{in}} = 100$ and $N = 26$, $R_{\text{in}} = 300$. As we mentioned in §6.2, it is possible to stop the rotation of the cylinder momentarily without experiencing a transition to a new mode. This procedure imposes a rather strong perturbation on the system. If the observed modes are unstable, they have an extremely long relaxation time and a large potential barrier separating them.

8. Discussion and conclusions

8.1. *Wave-number selection*

These experiments show that the non-uniqueness described by Coles (1965) also occurs in singly periodic flows. Evidence has been presented to show that both Coles' results and the present data are not strongly influenced by end and length effects. At least, these effects can be removed by corrections. It is also shown that, for a given mode (N, $m = 0$), the dependence of the observed wavelength on R_{in} is linear and the slope is exceedingly small. The slope is the same for all $(N, 0)$ for which the λ does not deviate too far from the linearized value. The wave-number always increases with R_{in}. No predictions of the wave-number at finite amplitude for rotating Couette flow are available for comparison.

The predictions of Schlüter *et al.* (1965) for the Bénard problem, of Ekhaus (1965) for the Poiseuille problem, of DiPrima (private communication) and Roberts (private communication) for the Couette problem, that there is a band of allowed wavelengths which is narrower than the band that can grow according to linear theory has been shown experimentally to be true for Couette flow. The calculations of Schlüter *et al.* indicate an asymmetry in the band width about the onset wave-number, with the increase occurring on the side of increasing a. We have observed this behaviour but hesitate to make a comparison because it is not known if the analogy between Bénard convection and the Taylor problem holds on this point.

Segel's (1962) suggestion that the past history of the system determines the selection of a wavelength from the allowed band has been shown to hold up to about twice the critical R_{in} in our apparatus. At larger values of R_{in} there are transitions which cannot be explained by Segel's results. It is believed that an analysis such as that of Davey *et al.* (1968) can be applied to these transitions.

The present work may be criticized on the grounds that, for a change $N \to N+1$ or $N+2$, the wavelength must change by 4 to 8 %. If the apparatus were longer and the gap smaller, the ideal case of a continuous range of accessible wave-numbers would be approached. We have discussed above the reason for the choice $\eta = \frac{1}{2}$. In maintaining this ratio, the principal limitation on the length to gap ratio is one of engineering and the second limitation is the cost. A solid rod of steel 1 m long will bend near its mid-point sufficiently to cause a variation of the gap by 1 % or more unless it has a diameter of 2·5 cm. At least this has been our experience. As the rod gets longer the diameter must be increased almost in proportion to prevent bending. There is no point in using longer cylinders. Glass and fixed dimensional plastics of precision bore with a length in excess of 1 m are

not available and must be custom made. We could increase the length to gap ratio by a factor of about 3 by making $R_1 \approx 1{\cdot}2$ cm, but we really need an order-of-magnitude increment to achieve a significant improvement. A rather sophisticated apparatus made of special materials with custom-made parts and costing an enormous amount appears to be the only way to push this type of investigation much farther.

8.2. *Adjustment time*

In §5 it was shown that after a change in the conditions of the apparatus the steady state is not re-established until about $\frac{1}{6}$ the diffusion time has elapsed. This period is much longer than the spin-up time. When considering geophysical processes in nature it is important to realize that some processes, such as the modification of secondary flow, take place on the diffusive time scale while mean motions are controlled by the spin-up time scale.

8.3. *Deterministic vs. statistical interpretation*

Our point of view toward the interpretation of the data is deterministic, not statistical. If the history of the boundary conditions is known, the final state can be predicted without qualification. An accessible state at R_{in} can be reached by starting the apparatus in a particular way and every time the apparatus is started in this way the same state will be reached. The history of the mean flow and that of the disturbance can be recorded with thermistor anemometers and our statement on determinancy is based upon such records. The observed indeterminancy only arises when the past history of the apparatus is not known. A statistical interpretation of the results is inappropriate because the past history has a lasting effect on the outcome. Statistical methods assume the influence of the initial value of the variables on the present value of the ensemble which is a transient and dies out as $t \to \infty$. Also, for the problem in hand there is no need to surrender to the less precise standards of statistical averages when complete solutions to the governing equations are easily realized. However, statistical methods are very useful in certain situations and the experimental work developed here may have some utility in studying the statistical mechanics of non-linear processes.

When we encounter an indeterminancy in non-linear systems, such as in the present problem, it is due to our neglect of the time variable. If the governing equations are simplified by dropping all time derivatives, the character of the equations is changed and it is not surprising that the character of the solution is changed.

Many non-linear systems, including the present case, have a manifold of solutions all satisfying the same boundary conditions. The bifurcation at onset for the Taylor problem is well known (Velte 1965). In the non-linear region the number of solutions increases as R_{in} gets larger. This is the important result of the theoretical work of Schlüter *et al.* (1965) (for the Bénard problem) and the experimental work of Coles (1965). The time variable tells us which solution is selected in a given observation.

In a recent inspiring lecture Professor Prigogine has commented on the existence of multiple, separate solutions in non-linear systems. The approach to

continuum problems which he outlined influenced the course of these experiments considerably. We believe the results of figure 8 show the multiple solutions due to non-linearity, as discussed by Prigogine, in the simplest case yet studied. These data also furnish an example of a many-body system in which the initial state has a lasting effect on the motion. If the motion described by figure 8 is sufficiently close to equilibrium so that the Prigogine–Resibois master equation holds (Prigogine 1962), then the persistent influence of the initial conditions prevents a Boltzman H-theorem from holding. It would be desirable to investigate two-dimensional rotating Couette flow by the methods of non-equilibrium statistical mechanics to find out how far these methods apply and what consequences the non-uniqueness has for statistical mechanics.

The remaining topic is a comparison of our results with the various extremum principles. The first point to be made is that the variational approach is not necessary. Ekhaus's method with a mixing of both wave-numbers and modes should predict the system's behaviour whenever R_{in} is close to and above the critical value. Since the theoretical work of Schlüter *et al.* and the experimental work presented here shows that a band of wave-numbers is equally stable, it is difficult to see how any extremum principle can be correct. It is a very strange flow, indeed, which has any extremum property over a range of flow patterns. For the problem in hand we have measured the torque and circulation in Taylor cells as their wavelength is changed while R_{in} is held fixed (Snyder 1968*a*). There is a measurable dependence of both quantities on a. A variational technique would pick one wavelength out of the observed range regardless of the initial conditions, and this result contradicts these experiments. We conclude that an extremum principle which is independent of time is not appropriate for wave-number selection in non-linear problems.

Comments on the first draft of this paper by Professors P. Roberts, L. Segel and especially R. C. DiPrima are gratefully acknowledged. At the time this paper was written the author was a visiting investigator at the Woods Hole Oceanographic Institution and the hospitality shown him by the staff is greatly appreciated. S. K. F. Karlsson and the author jointly maintain the equipment with which these data were taken at Brown University. The work was initiated by funds from Contract AF 19(628)-4783 with the Air Force Cambridge Research Laboratories, Office of Aerospace Research, and was continued under grants from the National Science Foundation: GK-1007 and GP-6344. The present research is supported by the Woods Hole Oceanographic Institution under Contract N00014-b6-C0241 with the Office of Naval Research. It is contribution no. 2038 from the Woods Hole Oceanographic Institution.

REFERENCES

CHANDRASEKHAR, S. 1961 *Hydrodynamic and Hydromagnetic Stability.* Oxford: Clarendon.

COLES, D. 1965 Transition in circular Couette flow. *J. Fluid Mech.* **21**, 385–425.

DAVEY, A. 1962 The growth of Taylor vortices in flow between rotating cylinders. *J. Fluid Mech.* **14**, 336–68.

DAVEY, A., DIPRIMA, R. C. & STUART, J. J. 1968 On the stability of Taylor vortices. *J. Fluid Mech.* **31**, 17–52.

DEARDORFF, J. W. & WILLIS, G. E. 1965 The effect of two-dimensionality on the suppression of thermal turbulence. *J. Fluid Mech.* **23**, 337–53.

DIPRIMA, R. C. 1967 Vector eigenfunction expansions for the growth of Taylor vortices in the flow between rotating cylinders. *Nonlinear Partial Differential Equations.* New York: Academic.

DONNELLY, R. J. & FULTZ, D. 1960 Experiments on the stability of viscous flow between rotating cylinders II. *Proc. Roy. Soc.* A **258**, 101–23.

DONNELLY, R. J. & SCHWARTZ, K. W. 1965 Experiments on the stability of viscous flow between rotating cylinders IV. *Proc. Roy. Soc.* A **283**, 531–46.

EKHAUS, W. 1965 *Studies in Non-Linear Stability Theory.* New York: Springer.

GLANSDORFF, P. & PRIGOGINE, I. 1964 On a general evolution criterion in macroscopic physics. *Physica*, **30**, 351–74.

GREENSPAN, H. P. & HOWARD, L. N. 1963 On a time-dependent motion of a rotating fluid. *J. Fluid Mech.* **17**, 385–404.

HAGERTY, W. W. 1946 Ph.D. dissertation, University of Michigan, Ann Arbor.

KOSCHMIEDER, E. L. 1966 On convection on a uniformly heated plate. *Beitr. Z. Phys. Atmos.* **39**, 1–11.

LAMBERT, R. B., SNYDER, H. A. & KARLSSON, S. K. F. 1965 Hot thermistor anemometer for finite amplitude stability measurements. *Rev. Sci. Instr.* **36**, 924–8.

MALKUS, W. V. R. & VERONIS, G. 1958 Finite amplitude cellular convection. *J. Fluid Mech.* **4**, 225–60.

MEYER, K. A. 1966 A two-dimensional time-dependent numerical study of rotational Couette flow. Ph.D. dissertation, Stanford University, Stanford.

PAI, S. I. 1943 *NACA TN* 892.

PRIGOGINE, I. 1962 *Non-equilibrium Statistical Mechanics.* New York: Interscience.

ROBERTS, P. H. 1965 Experiments on the stability of viscous flow between rotating cylinders: Appendix. *Proc. Roy. Soc.* A **283**, 531–46.

ROBERTS, P. H. 1966 On non-linear Bénard convection. *Non-equilibrium Thermodynamics, Variational Techniques, and Stability*, edited by R. J. Donnelly, R. Herman & I. Prigogine. University of Chicago Press.

ROSSBY, H. T. 1966 An experimental study of Bénard convection with and without rotation. Scientific Report HRF/SR27 Massachusetts Institute of Technology.

SCHLÜTER, A., LORTZ, D. & BUSSE, F. 1965 On the stability of steady finite amplitude convection. *J. Fluid Mech.* **23**, 129–44.

SEGEL, L. A. 1962 The non-linear interaction of two disturbances in the thermal convection problem. *J. Fluid Mech.* **14**, 97–114.

SEGEL, L. A. 1965 The non-linear interaction of a finite number of disturbances to a layer of fluid heated from below. *J. Fluid Mech.* **21**, 359–84.

SEGEL, L. A. 1966 Non-linear hydrodynamic stability theory and its application to thermal convection and curved flows. *Non-equilibrium Thermodynamics, Variational Techniques, and Stability*, edited by R. J. Donnelly, R. Herman & I. Prigogine. University of Chicago Press.

SNYDER, H. A. 1968*a* Change in wave-form and mean flow associated with wavelength variations in rotating Couette flow. Part 1. *J. Fluid Mech.* **35**, 337.

SNYDER, H. A. 1968*b* Stability of rotating Couette flow. Part I. Asymmetric waveforms. *Phys. Fluids*, **11**, 728.

SNYDER, H. A. & KARLSSON, S. K. F. 1964 Experiments on the stability of Couette motion with a radial thermal gradient. *Phys. Fluids*, **7**, 1696–1706.

SNYDER, H. A. & LAMBERT, R. B. 1966 Harmonic generation in Taylor vortices between rotating cylinders. *J. Fluid Mech.* **26**, 545–62.

STOMMEL, H. 1947 A summary of the theory of convection cells. *Ann. N.Y. Acad. Sci.* **48**, 715.

STUART, J. T. 1960 Non-linear effects in hydrodynamic stability. *Proc. Tenth Inter. Cong. Appl. Mech.* Stresa: Elsevier.

TAYLOR, G. I. 1923 Stability of a viscous liquid contained between two rotating cylinders. *Phil. Trans.* A **223**, 289–343.

VELTE, W. 1965 Stabilitätsverhalten und Verzweigung stationärer Lösungen der Navier–Stokesschen Gleichungen. *Arch. Rational Mech. Anal.* **16**, 97–125.